

Observation of hydrogen distribution in high-strength steel

G. KATANO, K. UEYAMA, M. MORI

Institute of Industrial Science, University of Tokyo, 7-22-1 Roppongi,

Minato-ku, Tokyo, 106-8558, Japan

E-mail: katano@post.kek.jp

“The diffusible hydrogen” in Cr-Mo steels are observed with autoradiography technique. Specimens with “the diffusible hydrogen” are prepared by an electrochemical cathodic charging method and those without “the diffusible hydrogen” by annealing at 373 K after charging hydrogen. TEM autoradiographs suggests, by the developed silver grains, that the hydrogen trapping sites are the grain boundary and internal interface of ferrite-cementite and ferrite-lath structure. After keeping the sample at 373 K, the silver grains disappeared. Most of hydrogen trapping sites release almost all the hydrogen at 373 K. It is clear that these sites of high-strength steels supplies “the diffusible hydrogen”. Hydrogen absorption characteristics of quench hardening tempering Cr-Mo steels have been evaluated by thermal desorption spectrometry (TDS). From tritium electron microscopic autoradiography and TDS analysis, the lower temperature (360 K–370 K) peaks show “the diffusing hydrogen” which is released a few days. “The diffusible hydrogen” from trapping sites such as the internal interface of ferrite-cementite or ferrite-lath structure are distinguished to “the diffusing hydrogen.” © 2001 Kluwer Academic Publishers

1. Introduction

High-strength steels are used for high tension bolt, aircraft, automobile components etc. Although these steels must meet stringent requirements with respect to strength, fracture toughness and resistance to environmentally assisted cracking, they are highly susceptible to delayed fracture (DF) caused by hydrogen embrittlement (HE).

The resistance of an alloy to HE is strongly affected by the interaction of hydrogen with microstructural heterogeneities that act as hydrogen traps [1]. The type of heterogeneity has a essential role in determining an alloy's intrinsic susceptibility to HE, with reversible (low binding energy) traps often imparting a high susceptibility. Therefore, characterization of alloys in terms of reversible trapping allows their intrinsic HE susceptibility to be assessed and provides a basis for examining the effect of traps on the observed resistance to HE.

The characterization of microstructural trapping of hydrogen in steels is essential to an improved understanding of HE. In the present work, tritium trapping sites in iron and high-strength steels have been observed by tritium autoradiography with scanning electron microscope (SEM) and with transmission electron microscope (TEM). Hydrogen thermal desorption spectroscopy (TDS) has been also applied for the study of hydrogen trapping in iron and steels [2–6]. Recently TDS method has been frequently employed because the DF problem exists for most high-strength steels. Specimens which are annealed at 464 K [2] or 473 K [3]

are not sensitive to the DF. This shows that hydrogen trapped with low binding energy plays an important role in DF and hydrogen trapped with high binding energy do not cause DF.

In the TDS experiment, hydrogen release peaks are observed at 385 K, 488 K and 578 K [4]. The peak at 385 K shows what is called “the diffusible hydrogen” and the other peaks show the trapping of hydrogen with high binding energy [5, 6].

Tritium electron microscopic autoradiography technique [7–9], which can visualize microscopic location near the surface where β -ray has been emitted by decay, has been applied to high-strength steels to investigate the behavior of hydrogen in steel. This can be performed by tritium TEM autoradiography because this method provides visual information about hydrogen distribution and microstructures in materials [7]. Hydrogen segregation at the grain boundary and microstructures in high-strength steel alloy is observed by means of tritium TEM autoradiography.

Observing “the diffusible hydrogen” with this technique is featured in this experiment. Specimens with “the diffusible hydrogen” are prepared by an electrochemical cathodic charging method and those without “the diffusible hydrogen” by annealing at 373 K after charging hydrogen. “The diffusible hydrogen” is trapped only weakly. Consequently “the diffusible hydrogen” can be released over a period of time at room temperature, and thus may be monitored by autoradiography for several weeks. On the other hand most of charged in hydrogen diffuse out of specimen

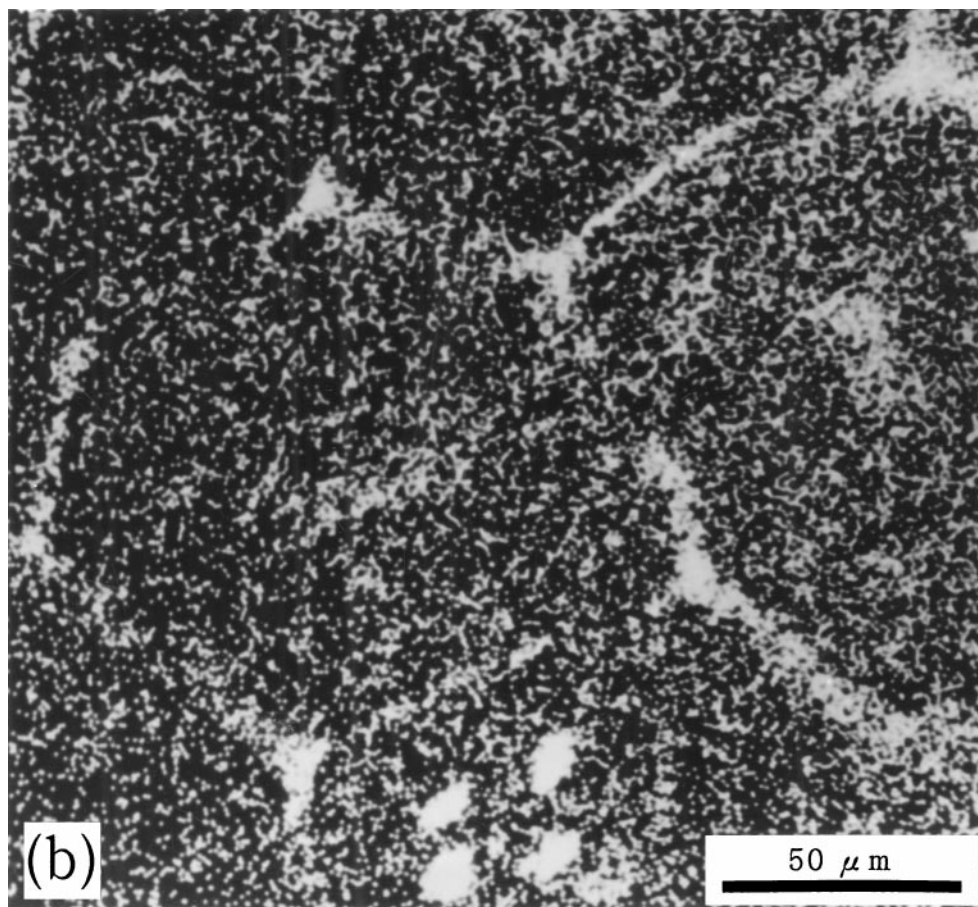
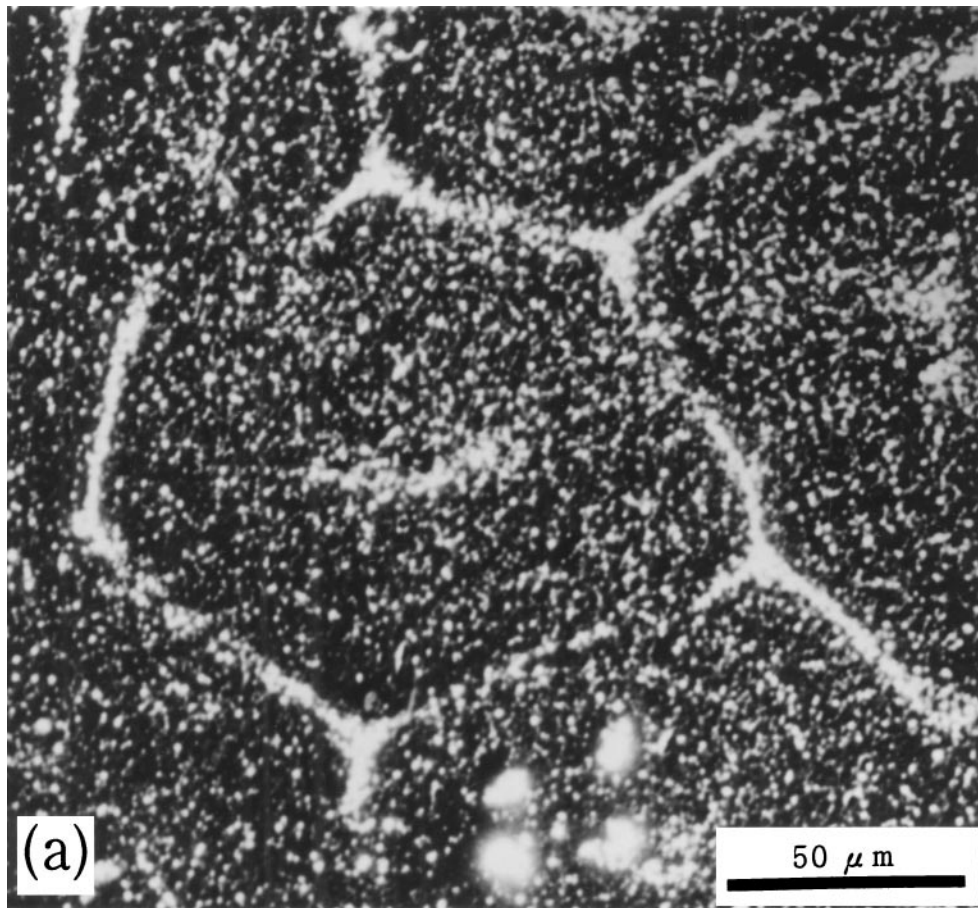


Figure 1 Tritium SEM autoradiographs of Cr-Mo steels : (a) SEM image of steel A (b) EPMA image of steel B (c) SEM image of steel B. Bright spots on SEM image show hydrogen distribution. EPMA show Ag image. (Continued).

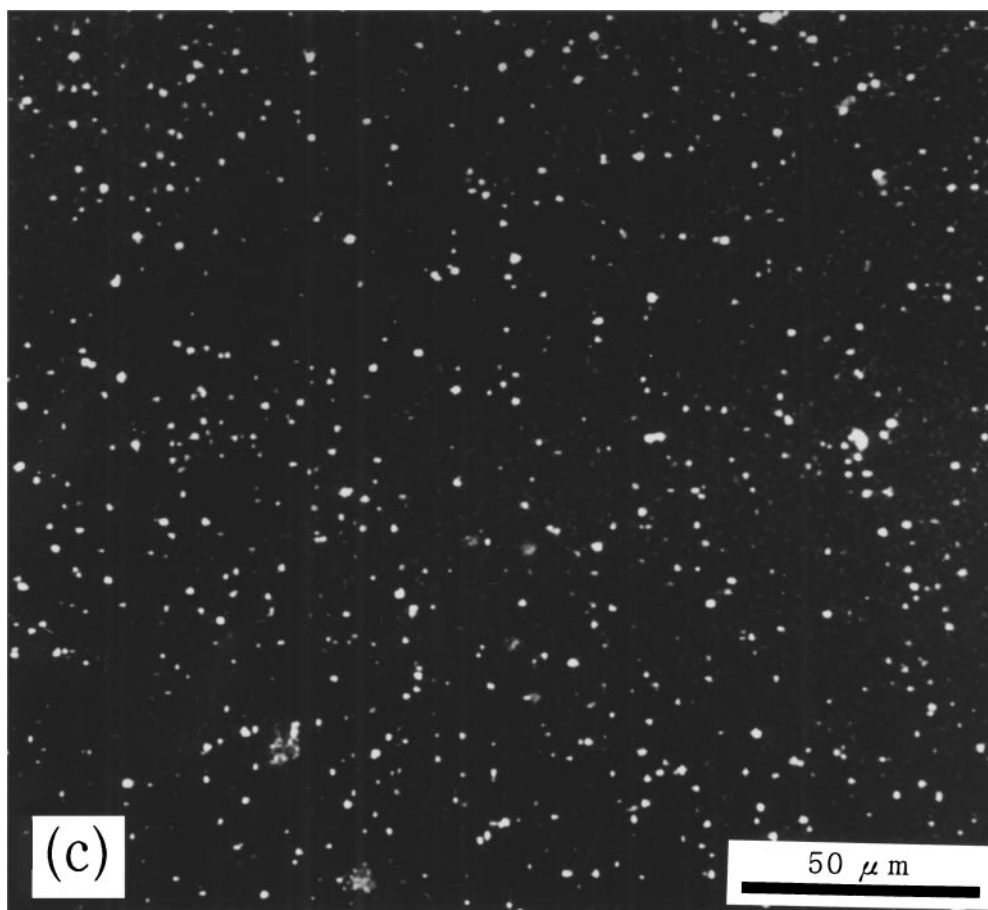


Figure 1 (Continued).

completely at room temperature during a few days. We distinguish to call this “the diffusing hydrogen.”

2. Experimental procedure

Two kinds of alloys Cr-Mo steels (A, B) are used in this study. Steel A is a commercial steel. Steel B is prepared from steel A by heat treatment, for comparison with steel A. Table I shows the composition and heat treatment of each steels. Steel A has a ferrite and cementite structure (tempered and martensite). Steel B a ferrite and ferrite-lath structure.

2.1. Electrochemical charging

For the TDS and autoradiographic experiment, hydrogen addition into the abraded specimens has been performed by an electrochemical cathodic charging method at room temperature. The electrolyte was 0.10 kmol/m^3 NaOH aqueous solution containing tritium of $3.7 \times 10^{15} \text{ Bq/m}^3$. The current density is 25 A/m^2 and the maximum charging time is 2.0 hours.

2.2. Autoradiography

Hydrogen (and tritium) charged specimens are kept at room temperature for 3 days to decrease “the diffusing hydrogen.” These are specimens with “the diffusible hydrogen.” Specimens without “the diffusible hydrogen” are prepared by annealing in an electric oven under helium atmosphere after electrochemical charging. The temperature is kept constant for one hour at 328 K or 373 K.

Specimens are dipped into liquid collodion (diethyl ether : ethanol : collodion = 6 : 6 : 1) and are desiccated. A monolayer of thin collodion film is made on the surface of specimens. A sensitive monogranular film of liquid photographic nuclear emulsion made of fine silver bromide grain (Ilford L4 ; $0.12 \mu\text{m}$ in diameter) is coated on this collodion. The specimen with sensitive film is placed in a dark box under nitrogen atmosphere maintained at 253 K. The film is exposed to β -rays emitted from the tritium in the specimen for 13 weeks. They are developed by D19 developer (Kodak). After chemical treatment, specimens are observed by SEM or TEM.

TABLE I The composition (mass %) and heat treatment of steels. (O.Q: oil quenching; W.Q: water quenching)

Steel	C	Si	Mn	P	S	Cr	Mo	Al	Heat Treatment
A	0.40	0.26	0.75	0.016	0.012	1.02	0.20	0.027	1128 K \times 30 min O.Q \rightarrow 743 K \times 60 min W.Q
B									1128 K \times 30 min O.Q

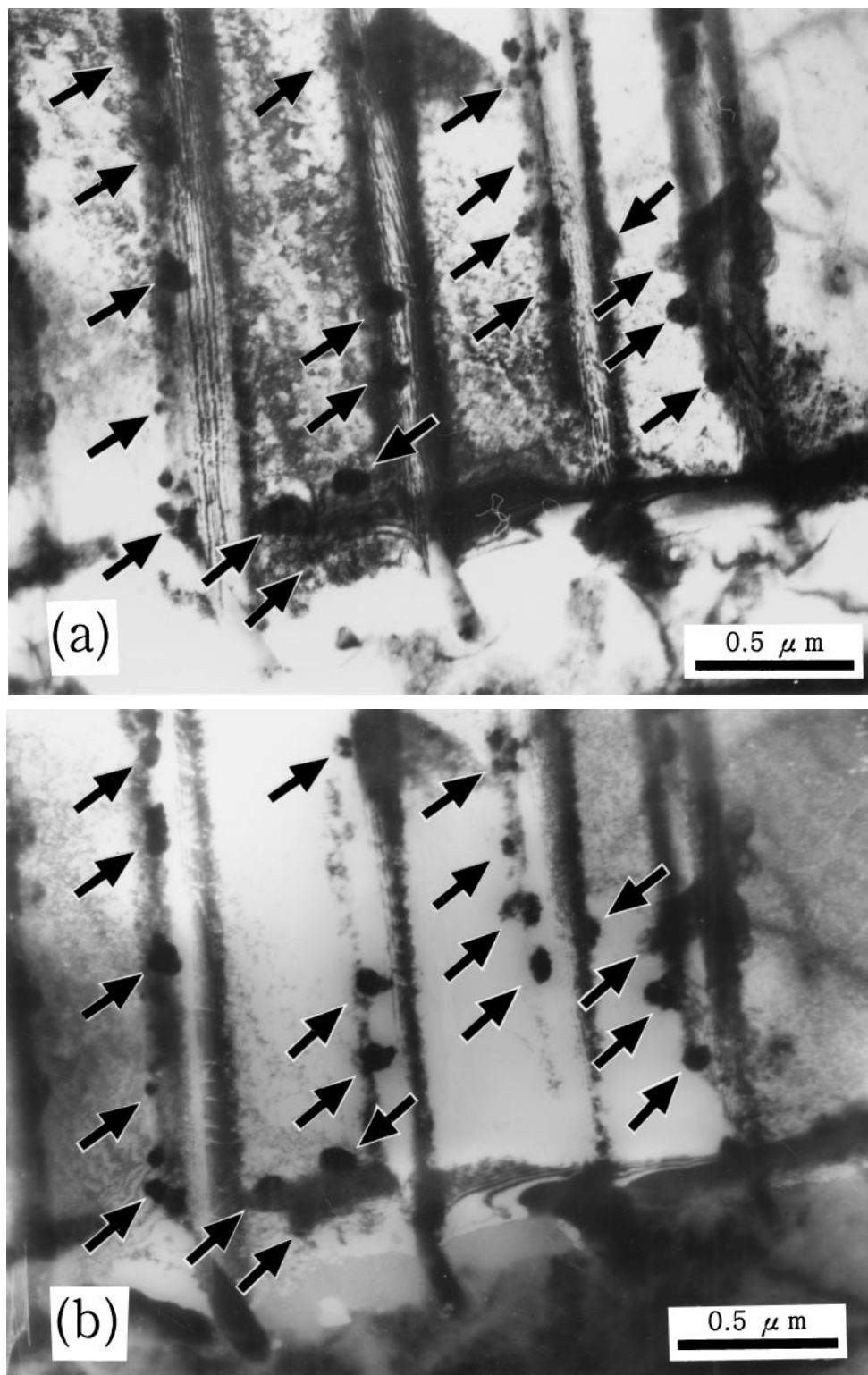


Figure 2 Tritium TEM autoradiographs and microstructures of Cr-Mo steels. Dark spots (by arrow signs) show Ag particles. (a) autoradiograph of steel A at bright field (b) autoradiograph of steel A at dark field. (c) microstructures of steel A: white zones are ferrite and black zones are cementite. (d) autoradiograph of steel B at bright field. (e) microstructures of steel B: stripes are lath structure. (Continued).

2.3. TDS

TDS of tritium is conducted immediately after charging. A sample is placed in a quartz tube and heated continuously at a standard heating rate of 10 K/min. Tritium desorbed from the sample are flown with helium gas and detected by a radiogas analyzer (Aloka RG-212) equipped with proportional counters. Propane is mixed with helium just before the entry into the detector. The

sampling time of the gas for successive measurements is 14.0 s.

3. Results and discussion

3.1. Autoradiography with "the diffusible hydrogen"

After exposure, the sensitive film on the specimen is developed to turn the silver bromide grains exposed by the

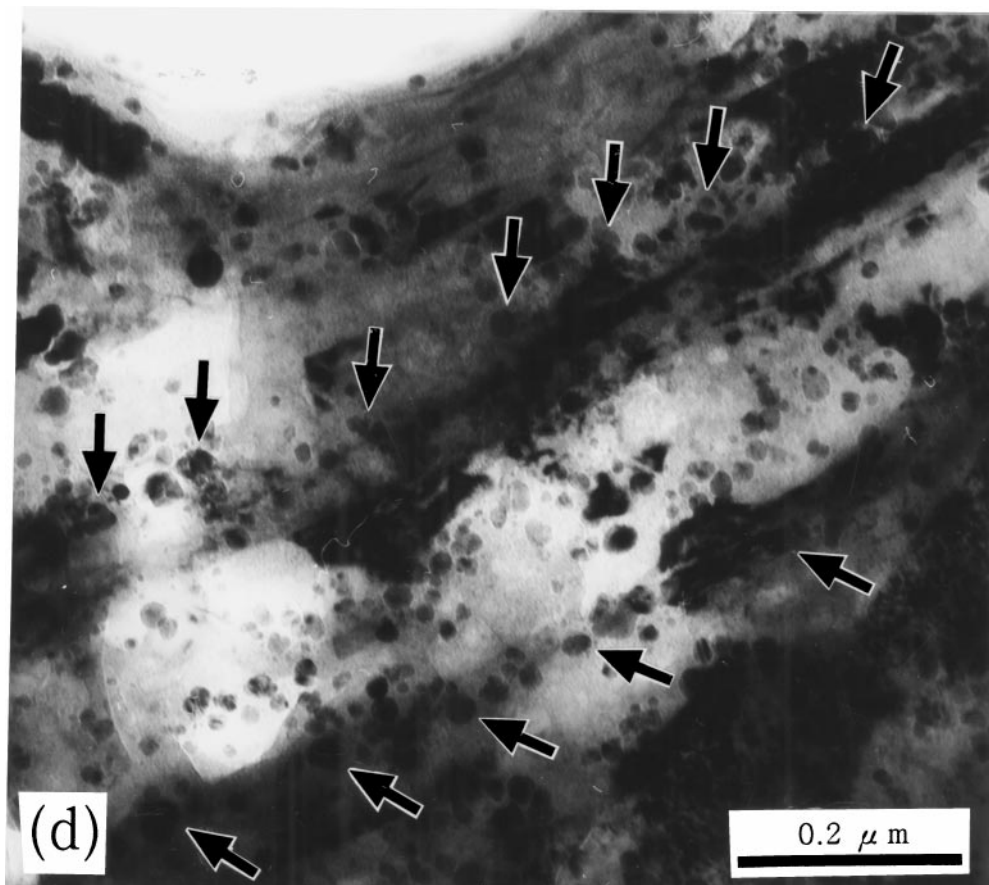
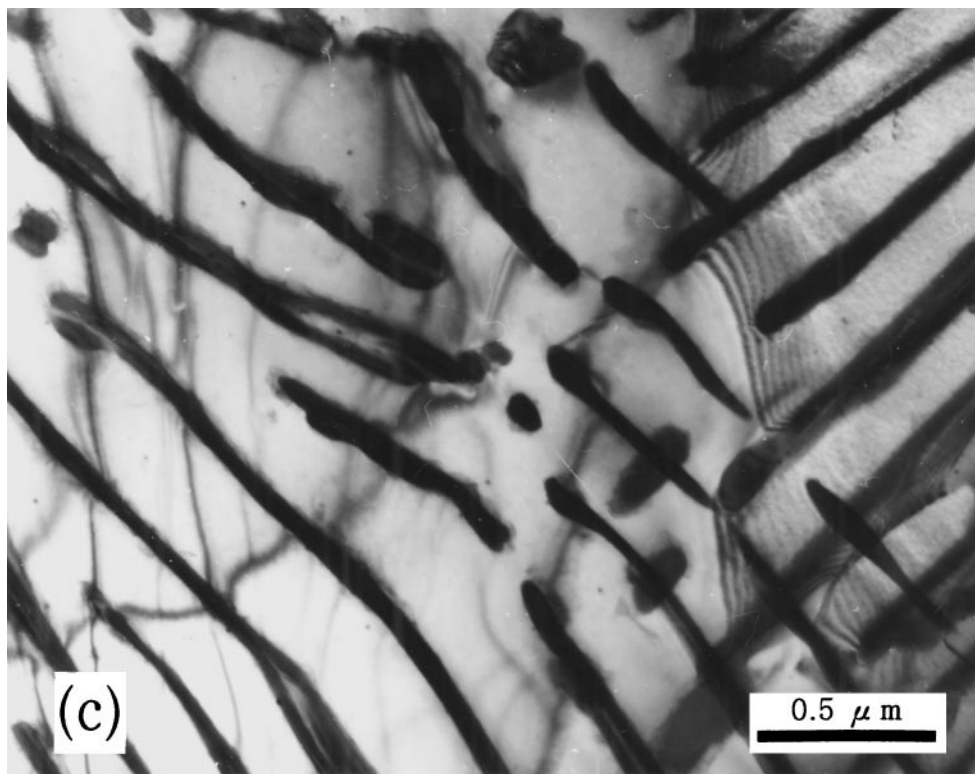


Figure 2 (Continued).

β -ray into metallic silver grains. Consequently the distribution of hydrogen in the specimen can be visualized as the distribution of silver grains in the autoradiograph. It is noted that the visualized hydrogen in the present autoradiograph is very low binding energy trapped hydrogen because “diffusing hydrogen” is fully released from the specimen.

Fig. 1 shows the tritium SEM autoradiograph of steels (A, B) subjected to a hydrogen charging time of 2.0 hours. In the SEM micrographs silver grains are observed as bright (white) spots. EPMA images show silver. Bright spots of SEM correspond to silver spots of EPMA. In contrast to this, in the tritium SEM autoradiograph of the two specimens with the same

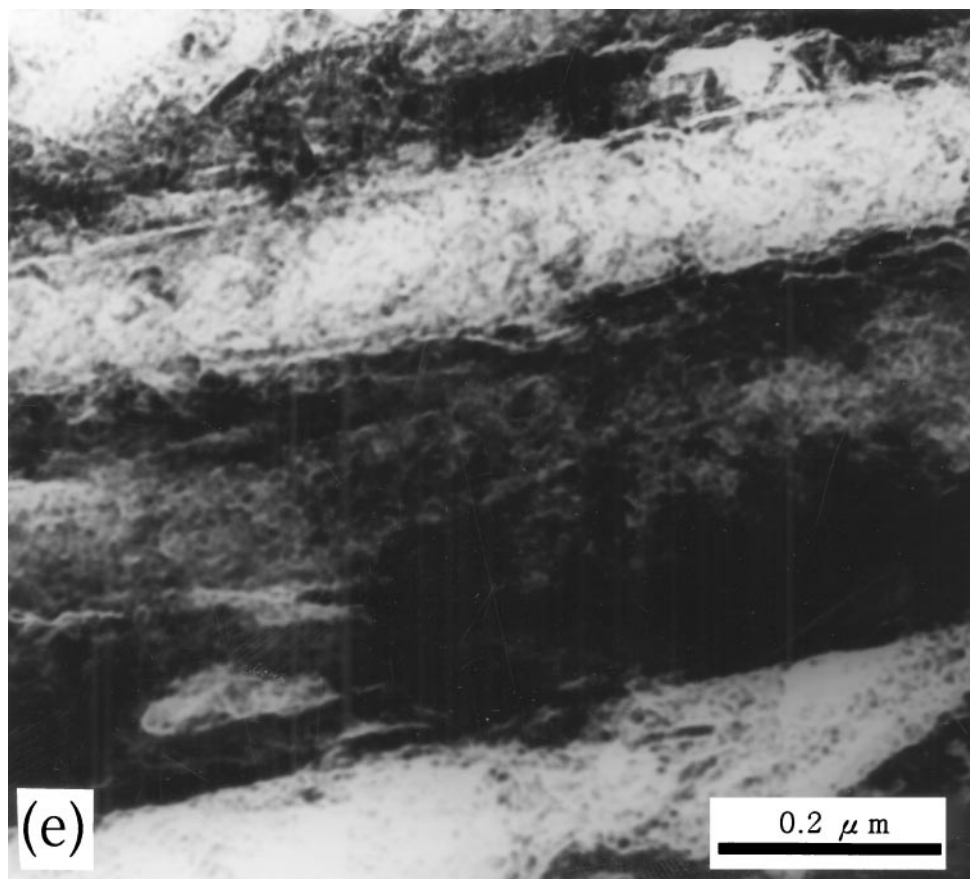


Figure 2 (Continued).

hydrogen charging time of 2.0 hours, steel A have accumulation of silver grains at the boundary, but steel B have no accumulation of silver grains appears.

Fig. 1a shows silver grains make cell structure and random distribution in cell. The cell structures show hydrogen in the grain boundary and the random distribution shows hydrogen in matrix. Thus the silver grains are located in the grains and are also segregated at the grain boundary. Especially around the grain boundary, the remaining hydrogen in these specimens is high concentration. On the other hand steel B (Fig. 1c), which did not receive the tempering heat treatment and, shows only random distribution.

Fig. 2 shows the tritium TEM autoradiograph of steels (A, B). In the TEM micrographs, silver grains are observed as dark (black) spots. In these photographs, white zones are ferrite structure and black zones are cementite (Fe_3C) or lath structure.

Fig. 2a is a photograph of steel A autoradiograph at bright field. The feature of micro structure is stripe which consists of ferrite and cementite alternately (Fig. 2c). Several dark spots (silver grains) are located in the internal interface of white zones and black zones. These dark spots are recognized as silver grains to compare with dark field image (Fig. 2b).

Fig. 2e is a photograph of steel B autoradiograph. Although similar stripes as steel A are observed, these are different. Bright zone and dark zone are both ferrites. These interface is called "lath boundary" which is internal interface between ferrites. Many silver grains are located in this lath boundary.

Although two steels have different microstructures, TEM autoradiographs show similar features of the silver grains. The silver grains are observed at the internal interface for both steels. Thus these microstructures which is the internal interface of ferrite-cementite or ferrite-lath are very important hydrogen trapping sites.

3.2. Autoradiography without "the diffusible hydrogen"

Fig. 3a shows the tritium SEM autoradiograph of steel A subjected to a hydrogen charging time of 2.0 hours and then kept at 328 K for 1.0 hour. Many silver grains are observed. However the number of silver grains is decreased compared with Fig. 1a.

Fig. 3b shows specimens kept at 373 K for 1.0 hour after charging. Almost no silver grains are observed. The cell structure is not observed either.

Silver grains which show trapped hydrogen at room temperature are observed in Fig. 3a, but not in Fig. 3b; which suggests that the trapped hydrogen in Fig. 3a is "the diffusible hydrogen."

Fig. 4 shows the TEM autoradiograph specimens of steels A with the same heat treatment condition as in Fig. 3. After keeping the sample at 328 K, some silver grains are observed. However, by keeping at 373 K, only few silver grains are observed. This suggests that the trapped hydrogen in the internal interface remains until 328 K, but escapes at 373 K. Fig. 4c shows steel B specimen keeping at 373 K, only few silver grains are observed in lath boundary either.

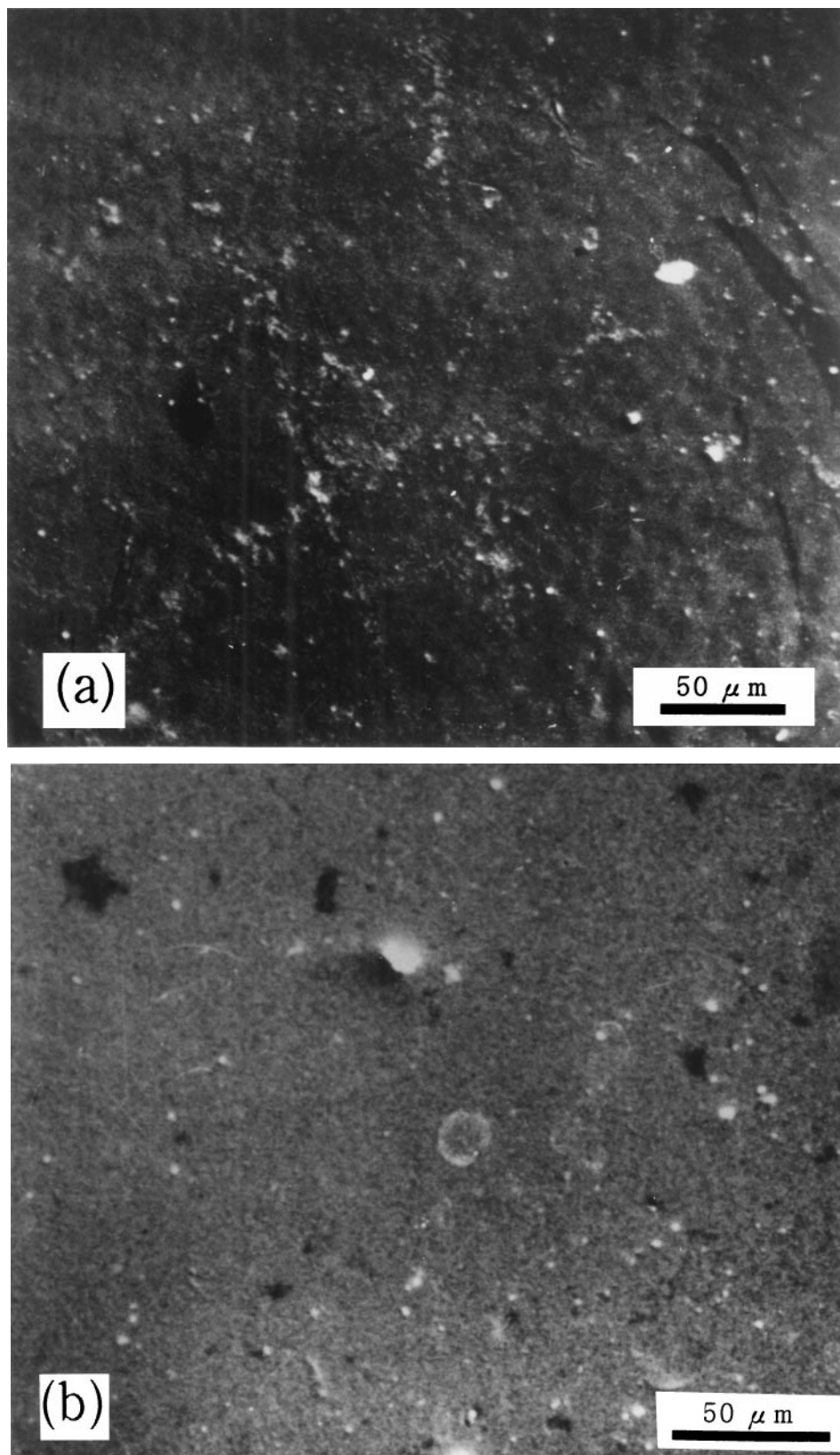


Figure 3 SEM autoradiography without “the diffusible hydrogen”: (a) steel A kept at 328 K (b) steel A kept at 373 K. Almost all Ag particles disappear.

In other words the decrease of silver grains in SEM autoradiographs is caused by releasing hydrogen from the internal interface. These hydrogen trapping sites have low binding energy. These sites can trap hydrogen with high concentration by an electrochemical charging. In atmosphere at room temperature, at least these sites keep a little hydrogen and trapped hy-

drogen are verified with tritium autoradiography. Thus the boundary of ferrite-cementite or ferrite-lath structure plays an important role in hydrogen trapping at room temperature. However by annealing the specimen at 373 K, these trapping sites release hydrogen. These results suggest the importance of “the diffusible hydrogen.”

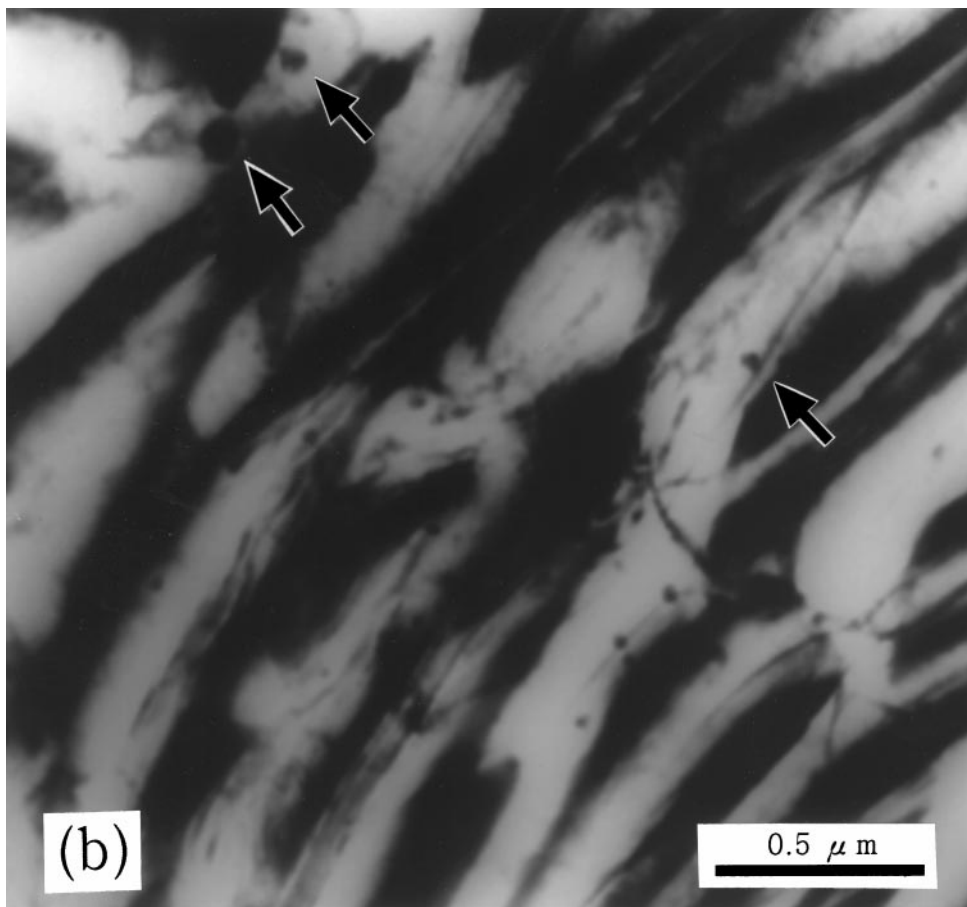
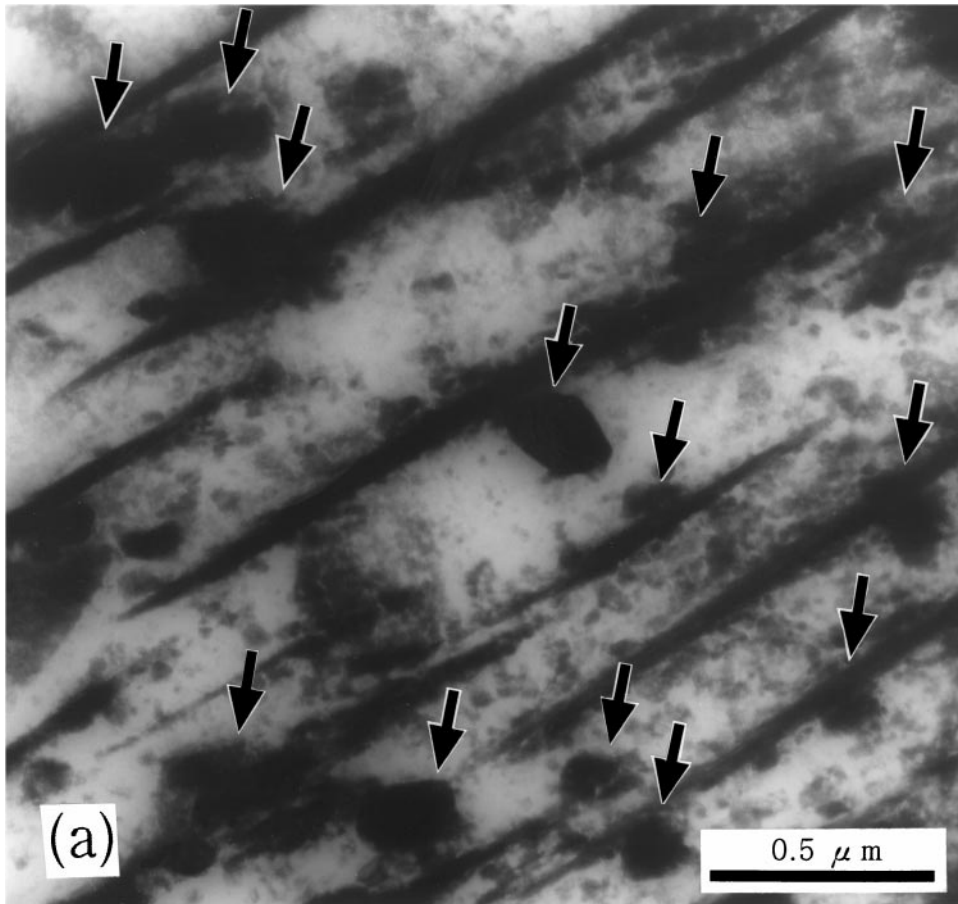


Figure 4 TEM autoradiographs without “the diffusible hydrogen”: (a) steel A kept at 328 K (b) steel A kept at 373 K (c) steel B kept at 373 K. (Continued).

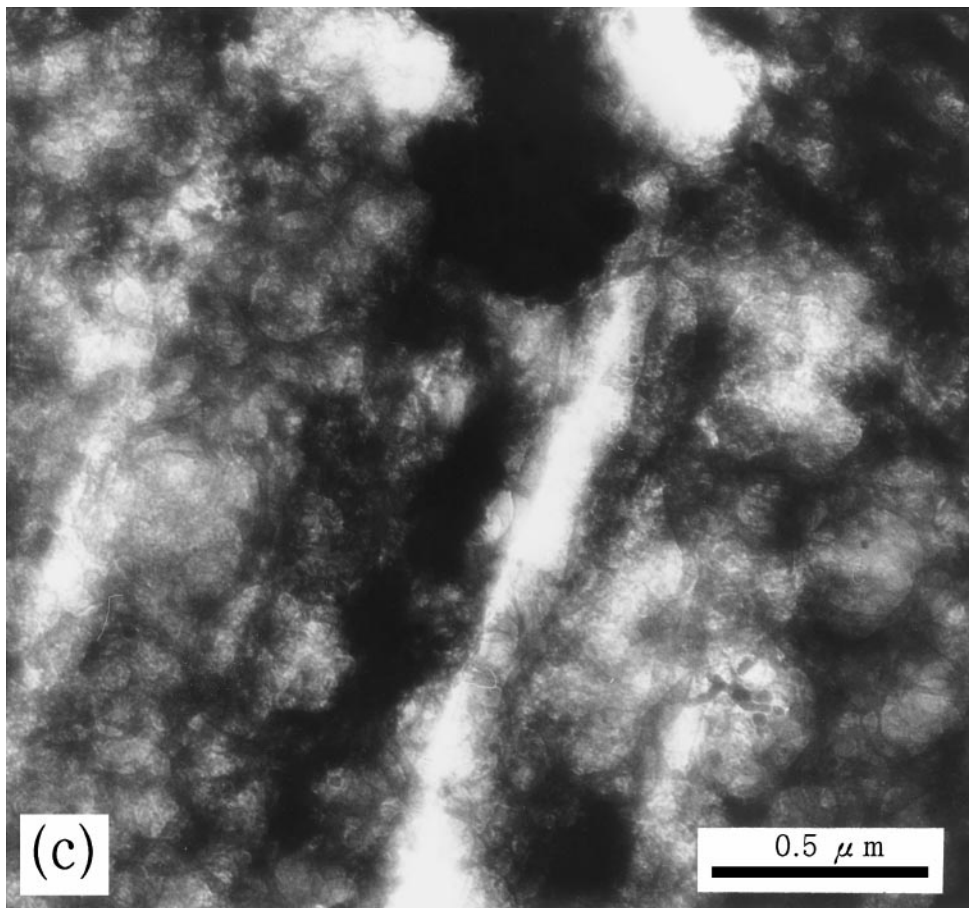


Figure 4 (Continued).

The distance between hydrogen trapping sites and grain boundary is an important factor for DF. HE arises from concentrated hydrogen at some defects. To gather hydrogen into these defects under the stress spends some period [10].

High-strength steels have hydrogen trap sites of low binding energy. These sites absorb hydrogen under moist atmosphere, water, hydrogen gas and corrosive gas or liquid etc., and release hydrogen under dry air or vacuum [11]. Hydrogen concentration in steels have fluctuated with environment.

Under the stress, hydrogen tends to gather into some defects [12]. Therefore the amount of hydrogen and distance from trap sites to these defects influence kinetics of gathering hydrogen and characteristic of the DF.

3.3. TDS

Fig. 5 shows the TDS releasing tritium spectra of the steels (A, B). The first peak appears in the temperature range between 360 K and 370 K. Fig. 5c shows the TDS spectra of steel A specimens kept at room temperature for 1 week. The first peak disappears, indicating that most of the hydrogen in specimens escapes from the surface by diffusion. It is clear that “the diffusing hydrogen” is detected with this TDS method and “the diffusible hydrogen” is detected with autoradiography method in this experiment.

The first peak tritium is mostly “the diffusing hydrogen,” because the tritium is released the period of one week after charging at room temperature. These tritium

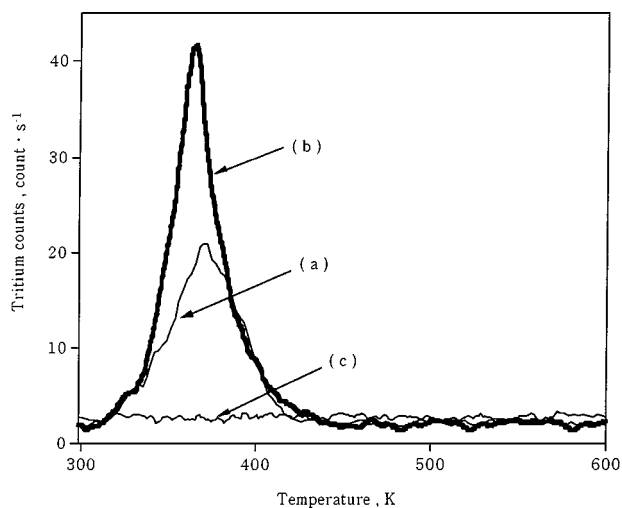


Figure 5 TDS spectra of the steels (A, B). (a) steel A (b) steel B (c) one week after charging at room temperature in steel A.

does not appear in the autoradiography after keeping room temperature for 3 days. In autoradiography, “the diffusible hydrogen” which remains for a longer time is shown. “The diffusible hydrogen” is trapped within several weeks or several months. Therefore “the diffusible hydrogen” appears in exposing the autoradiography specimens. The autoradiography can detect a very small amount of “the diffusible hydrogen” which the proportional counter can not be measured in this TDS method.

4. Conclusions

The present experimental results are summarized as follows:

1. SEM autoradiographs at room temperature show that the silver grains are located in the grains and the grain boundaries in the tempering martensite steel. TEM autoradiographs suggests that the hydrogen trapping sites in the grains are the internal interface of ferrite-cementite and ferrite-lath structure.

2. After keeping the sample at 373 K, the silver grains disappeared mostly. The internal interface sites release almost all the hydrogen at 373 K. It is clear that these sites of high-strength steels supplies “the diffusible hydrogen.”

3. Thermal desorption of tritium charged into Cr-Mo steels specimens mostly took place in first peak temperature range between 360 K and 370 K. These peaks disappear in 1 week after charging tritium. Almost all hydrogen is “the diffusing hydrogen.”

References

1. I. M. BERNSTEIN and G. M. PRESSOUYRE, in “Hydrogen Degradation of Ferrous Alloys,” edited by R. A. Oriani, J. P. Hirth

- and M. Smialowski. (Noyes Publications, Park Ridge, New Jersey, 1985) p. 641.
2. H. E. TOWNSEND, *Corrosion NACE* **37** (1981) 115.
3. N. SUZUKI, N. ISHI and T. MIYAGAWA, *TETUTOHAGANE* **82** (1996) 170.
4. W. Y. CHOO and J. Y. LEE, *Metall. Trans.* **13A** (1982) 135.
5. K. TAKAI, G. YAMAUCHI, M. NAKAMURA and M. NAGUMO, *J. Japan Inst. Metals* **62** (1998) 267.
6. M. NAGUMO, K. OHTA and H. SAITO, *Scripta Mater.* **40** (1999) 313.
7. H. SAITO, K. MIYAZAWA and Y. ISHIDA, *J. Japan Inst. Metals* **55** (1991) 366.
8. M. NAGUMO, *Bull. Japan Inst. Metals* **21** (1982) 672.
9. T. ASAOKA, G. LAPASSET, M. AUCOUTURIER and P. LACOMBE, *Corrosion* **34** (1978) 39.
10. H. H. JOHNSON, J. G. MORLET and A. R. TROIANO, *Trans. AIME* **212** (1958) 526.
11. N. SUZUKI, N. ISHI, T. MIYAGAWA and H. HARADA, *TETUTOHAGANE* **79** (1993) 227.
12. G. ITOH, N. HARAMURA and T. IHARA, *J. Japan Inst. Metals* **63** (1999) 593.

Received 10 March

and accepted 4 October 2000